



Research paper

Homoleptic complexes of divalent metals bearing *N,O*-bidentate imidazo [1,5-*a*]pyridine ligands: Synthesis, X-ray characterization and catalytic activity in the Heck reaction

G. Attilio Ardizzoia^a, Daniel Ghiotti^a, Bruno Therrien^b, Stefano Brenna^{a,*}^a *University of Insubria, Department of Science and High Technology and CIRCC, Via Valleggio 9, 22100 Como, Italy*^b *Institute of Chemistry, University of Neuchâtel, Avenue de Bellevaux 51, CH-2000 Neuchâtel, Switzerland*

ARTICLE INFO

Article history:

Received 13 July 2017

Received in revised form 18 September 2017

Accepted 22 November 2017

Available online 24 November 2017

Keywords:

Heck reaction

N,O-ligandsImidazo[1,5-*a*]pyridine

Crystal structure

Homogeneous catalysis

DFT calculations

ABSTRACT

Two imidazo[1,5-*a*]pyridine-based ligands, namely 2-(1-phenylimidazo[1,5-*a*]pyridin-3-yl)phenol (N,OH-L^{Ph}) and 2-(1-methylimidazo[1,5-*a*]pyridin-3-yl)phenol (N,OH-L^{Me}) have been reacted with different divalent metals (M = Co, Cu, Ni, Pd) to obtain the following complexes [Co(N,O-L^{Ph})₂] (1), [Cu(N,O-L^{Ph})₂] (2), [Ni(N,O-L^{Ph})₂] (3), [Pd(N,O-L^{Ph})₂] (4), [Co(N,O-L^{Me})₂] (5), [Cu(N,O-L^{Me})₂] (6), [Ni(N,O-L^{Me})₂] (7) and [Pd(N,O-L^{Me})₂] (8). These homoleptic complexes showed the monoanionic ligands to be coordinated in a *N,O*-bidentate mode via the pyridine-like nitrogen of the imidazo[1,5-*a*]pyridine skeleton and the phenolic oxygen. The coordination mode of the ligands was confirmed by the single-crystal X-ray structure analysis of [Co(N,O-L^{Ph})₂] (1) and [Pd(N,O-L^{Me})₂] (8). The palladium compounds [Pd(N,O-L^{Ph})₂] (4) and [Pd(N,O-L^{Me})₂] (8) proved to be good catalysts in the Heck reaction between iodobenzene and different olefins.

© 2017 Elsevier B.V. All rights reserved.

1. Introduction

One of the most powerful C–C bond forming transformation is the Mizoroki-Heck reaction [1,2] which was originally proposed as the coupling between aryl or vinyl halides and activated alkenes, in the presence of a base. Since then this reaction has been intensively investigated and nowadays a broader range of both intermolecular [3–5] and intramolecular [6] versions are available. The use of chiral ligands also allowed for asymmetric [7–9] Heck couplings to take place. The Heck reaction is usually catalyzed by palladium and involves a Pd(0)/Pd(II) cycle [10,11]. However, recent examples on the use of different palladium(II) catalysts which work with a Pd(II)/Pd(IV) cycle [12,13] or even other transition metals like cobalt, copper or nickel [14] have been reported in the literature.

Imidazo[1,5-*a*]pyridines constitute a very important class of heterocyclic compounds [15–19] whose interesting photochemical and biological properties are widely known in the literature. They find application in several fields of research, from pharmaceutical uses based on their antiviral [20] or antibacterial [21] activities to utilization in Organic Light Emitting Diodes (OLEDs) [22–24] or thin-layer Field Effect Transistors (FET) [25]. In particular, they

recently emerged as low cost emitters with large Stokes' shift [26] and as potential ligands in the synthesis of luminescent transition metal compounds [27–31]. Finally, imidazo [1,5-*a*]pyridine-based complexes have been recently employed as catalysts in olefin epoxidation [32] or transfer hydrogenation of ketones [33].

In the past, we widely explored the coordination chemistry of *N*-based multidentate ligands [34–37], with special attention to pyrazole and its analogues (imidazole, triazole) both in their neutral [38–40] and anionic azolate forms [41]. In this investigation on *N*-based ligands, we lately conducted a study on the photophysical properties of zinc(II) [42–43] and silver(I) [44] compounds with 3-aryl-substituted 1-pyridylimidazo [1,5-*a*]pyridines. In these luminescent complexes, the imidazo-pyridine ligands coordinate to the metal centers with the pyridine ring (N_{py}) and the pyridine-like nitrogen of the imidazo[1,5-*a*]pyridine group (N_{im}), thus acting as *N,N*-bidentate neutral ligands. In this context, herein we employed two similar ligands, 2-(1-phenylimidazo[1,5-*a*]pyridin-3-yl)phenol (N,OH-L^{Ph}) and 2-(1-methylimidazo[1,5-*a*]pyridin-3-yl)phenol (N,OH-L^{Me}) to synthesize complexes of divalent metals. As established by X-ray diffraction analysis, the anionic form of N,OH-L^{Ph} and N,OH-L^{Me} coordinate to the metal centers in a *N,O*-bidentate mode. The synthesized compounds were used as catalysts in the Heck reaction, showing good catalytic activity in the

* Corresponding author.

E-mail address: stefano.brenna@uninsubria.it (S. Brenna).

intermolecular coupling between iodobenzene and different olefins in the case of Pd-containing derivatives.

2. Experimental

2.1. Materials and methods

All reactions were carried out under purified nitrogen using standard Schlenk techniques. Solvents were dried and distilled according to standard procedures prior to use. NMR spectra were recorded with an AVANCE 400 Bruker spectrometer at 400 MHz for ^1H NMR and 100 MHz for $^{13}\text{C}\{^1\text{H}\}$ NMR. Chemical shifts are given as δ values in ppm relative to residual solvent peaks as the internal reference. Elemental analyses were obtained with a Perkin-Elmer CHN Analyzer 2400 Series II. Infrared Spectra were acquired on a Shimadzu Prestige 21 instrument with a 1-cm^{-1} resolution. ATR-IR Spectra were acquired on a Nicolet iS10 FT-IR instrument equipped with Smart iTR ATR accessory with a 1-cm^{-1} resolution. Quantitative analyses of products in the catalytic runs were performed on a Finningan Trace GC with a DB-5MS UI capillary column (30 m, 0.25 mm) equipped with a Finningan Trace Mass Spectrometer. Ligand 2-(1-phenylimidazo[1,5-*a*]pyridin-3-yl)phenol (N,OH- L^{Ph}) was prepared according to literature methods [45,27], whereas 2-(1-methylimidazo[1,5-*a*]pyridin-3-yl)phenol (N,OH- L^{Me}) was prepared by a slight modification of the same procedure. All other chemicals were of reagent grade quality from commercial sources (Aldrich, TCI Chemicals) and used as received.

2.2. Syntheses

2.2.1. Synthesis of ligand N,OH- L^{Me}

A mixture of 2-acetylpyridine (1 mL, 8.92 mmol, 1 eq), salicylaldehyde (1.9 mL, 17.83 mmol, 2 eq) and ammonium acetate (3.44 g, 44.58 mmol, 5 eq) in glacial acetic acid (30 mL) was stirred at room temperature for 7 days. Then the mixture was poured into 150 mL of water and extracted with CH_2Cl_2 (200 mL). The organic phase was washed with a saturated aqueous solution of NaHCO_3 , dried with Na_2SO_4 and the suspension was filtered. The solvent was evaporated under vacuum, and the crude product was crystallized with hexane. Yield: 1.915 g (75%). Anal. Calcd for $\text{C}_{14}\text{H}_{12}\text{N}_2\text{O}$ (%): C, 74.98; H, 5.39; N, 12.49. Found (%): C, 74.66; H, 5.31; N, 12.08. ^1H NMR (400 MHz, CDCl_3): δ 12.48 (s, 1H), 8.92 (d, 1H, $J = 7.3$ Hz), 8.28 (d, 1H, $J = 7.8$ Hz), 8.01 (d, 1H, $J = 9.1$ Hz), 7.87 – 7.78 (m, 1H), 7.73 (d, 1H, $J = 8.1$ Hz), 7.54 (t, 1H, $J = 7.6$ Hz), 7.30 (t, 1H, $J = 6.3$ Hz), 7.20 (t, 1H, $J = 6.9$ Hz), 3.15 (s, 3H).

2.2.2. Synthesis of $[\text{Co}(\text{N},\text{O}-L^{\text{Ph}})_2]$ (1)

A suspension of $\text{CoCl}_2 \cdot 6\text{H}_2\text{O}$ (0.120 g, 0.504 mmol) and ligand N,OH- L^{Ph} (0.300 g, 1.048 mmol) in acetonitrile (15 mL) was treated with Et_3N (180 μL , 1.294 mmol). An orange-to-brown suspension formed, which was stirred at room temperature for 2 h. Then it was filtered and the solid washed with water, acetonitrile and diethylether to give a light brown product. Yield: 0.304 g (96%). Anal. Calcd for $\text{C}_{38}\text{H}_{26}\text{CoN}_4\text{O}_2$ (%): C, 72.49; H, 4.16; N, 8.90. Found (%): C, 71.99; H, 4.44; N, 8.79. X-ray quality single crystals ($1\text{C}_2\text{H}_4\text{Cl}_2$) were grown by slow diffusion of hexane into a 1,2-dichloroethane solution of 1.

2.2.3. Synthesis of $[\text{Cu}(\text{N},\text{O}-L^{\text{Ph}})_2]$ (2)

A suspension of anhydrous CuCl_2 (0.340 g, 2.827 mmol) and ligand N,OH- L^{Ph} (1.700 g, 5.937 mmol) in acetonitrile (40 mL) was treated with Et_3N (1.0 mL, 7.188 mmol). The suspension was stirred at room temperature for 2 h, then it was filtered and the solid washed with water, acetonitrile and diethylether to give a light grey product. Yield: 1.344 g (75%). Anal. Calcd for

$\text{C}_{38}\text{H}_{26}\text{CuN}_4\text{O}_2$ (%): C, 71.97; H, 4.13; N, 8.83. Found (%): C, 72.10; H, 4.32; N, 8.88.

2.2.4. Synthesis of $[\text{Ni}(\text{N},\text{O}-L^{\text{Ph}})_2]$ (3)

A suspension of $\text{NiCl}_2 \cdot 6\text{H}_2\text{O}$ (0.195 g, 0.820 mmol) and ligand N,OH- L^{Ph} (0.495 g, 1.729 mmol) in acetonitrile (15 mL) was treated with Et_3N (290 μL , 2.859 mmol). A yellow suspension formed, which was stirred at room temperature for 12 h. Then it was filtered and the solid washed with water, acetonitrile and diethylether to give a yellow product. Yield: 0.370 g (72%). Anal. Calcd for $\text{C}_{38}\text{H}_{26}\text{NiN}_4\text{O}_2$ (%): C, 72.52; H, 4.16; N, 8.90. Found (%): C, 72.66; H, 4.35; N, 8.93.

2.2.5. Synthesis of $[\text{Pd}(\text{N},\text{O}-L^{\text{Ph}})_2]$ (4)

A suspension of K_2PdCl_4 (0.150 g, 0.460 mmol) and ligand N,OH- L^{Ph} (0.280 g, 0.978 mmol) in dichloromethane (10 mL) was treated with Et_3N (220 μL , 1.602 mmol). The addition of the base slowly afforded a dark orange solution, which was stirred at room temperature for 3 days. Then the white solid (KCl) was removed by filtration over a pad of Celite, and the filtrate was evaporated to dryness. The resulting crude product was suspended in water, the suspension was filtered and the orange solid washed with diethylether. Yield: 0.258 g (83%). Anal. Calcd for $\text{C}_{38}\text{H}_{26}\text{N}_4\text{O}_2\text{Pd}$ (%): C, 67.41; H, 3.87; N, 8.28. Found (%): C, 66.99; H, 4.60; N, 8.41.

2.2.6. Synthesis of $[\text{Co}(\text{N},\text{O}-L^{\text{Me}})_2]$ (5)

A suspension of $\text{CoCl}_2 \cdot 6\text{H}_2\text{O}$ (0.100 g, 0.365 mmol) and ligand N,OH- L^{Me} (0.175 g, 0.780 mmol) in acetonitrile (15 mL) was treated with Et_3N (130 μL , 0.934 mmol). The resulting light brown suspension was stirred at room temperature for 2 h. Then it was filtered and the solid washed with water, acetonitrile and diethylether to give a light brown product. Yield: 0.120 g (66%). Anal. Calcd for $\text{C}_{28}\text{H}_{22}\text{CoN}_4\text{O}_2$ (%): C, 66.54; H, 4.39; N, 11.08. Found (%): C, 66.78; H, 4.43; N, 11.17.

2.2.7. Synthesis of $[\text{Cu}(\text{N},\text{O}-L^{\text{Me}})_2]$ (6)

A suspension of anhydrous CuCl_2 (0.250 g, 1.859 mmol) and ligand N,OH- L^{Me} (0.875 g, 3.902 mmol) in acetonitrile (30 mL) was treated with Et_3N (0.660 mL, 4.744 mmol). After stirring the suspension at room temperature for 2 h, it was filtered and the solid washed with water, acetonitrile and diethylether to give a light grey product. Yield: 0.650 g (68%). Anal. Calcd for $\text{C}_{28}\text{H}_{22}\text{CuN}_4\text{O}_2$ (%): C, 65.94; H, 4.35; N, 10.98. Found (%): C, 65.72; H, 4.21; N, 10.71.

2.2.8. Synthesis of $[\text{Ni}(\text{N},\text{O}-L^{\text{Me}})_2]$ (7)

A suspension of $\text{NiCl}_2 \cdot 6\text{H}_2\text{O}$ (0.195 g, 0.820 mmol) and ligand N,OH- L^{Me} (0.390 g, 1.739 mmol) in acetonitrile (15 mL) was treated with Et_3N (290 μL , 2.859 mmol). The resulting yellow suspension was stirred at room temperature for 12 h, then it was filtered and the solid washed with water, acetonitrile and diethylether to give a yellow product. Yield: 0.290 g (70%). Anal. Calcd for $\text{C}_{28}\text{H}_{22}\text{NiN}_4\text{O}_2$ (%): C, 66.57; H, 4.39; N, 11.09. Found (%): C, 66.38; H, 4.12; N, 10.87.

2.2.9. Synthesis of $[\text{Pd}(\text{N},\text{O}-L^{\text{Me}})_2]$ (8)

A suspension of K_2PdCl_4 (0.150 g, 0.460 mmol) and ligand N,OH- L^{Me} (0.220 g, 0.978 mmol) in dichloromethane (10 mL) was treated with Et_3N (220 μL , 1.602 mmol). The addition of the base afforded a dark solution, which was stirred at room temperature for 3 days. Then the white solid (KCl) was removed by filtration over a pad of Celite, and the filtrate was evaporated to dryness. The resulting crude product was suspended in water, the suspension was filtered and the orange solid washed with diethylether. Yield: 0.198 g (78%). Anal. Calcd for $\text{C}_{28}\text{H}_{22}\text{N}_4\text{O}_2\text{Pd}$ (%): C, 60.82; H, 4.01; N, 10.13. Found (%): C, 60.92; H, 4.33; N, 10.38. (NMR data

refer to the major isomer, see text) ^1H NMR (400 MHz, CD_2Cl_2): δ 8.36 (d, 1H, $J = 7.3$ Hz), 7.68 (d, 1H, $J = 8.0$ Hz), 7.38 (d, 1H, $J = 9.3$ Hz), 7.18 (t, 1H, $J = 8.0$ Hz), 6.99 (d, 1H, $J = 8.2$ Hz), 6.90 (t, 1H, $J = 7.5$ Hz), 6.64 (dd, 1H, $J = 9.1$ Hz, $J = 6.3$ Hz), 6.55 (t, 1H, $J = 6.8$ Hz), 2.46 (s, 3H). $^{13}\text{C}\{^1\text{H}\}$ NMR (100 MHz, CD_2Cl_2): δ 155.63, 133.47, 129.22, 126.62, 126.20, 123.84, 122.10, 118.75, 118.49, 117.87, 117.42, 113.71, 113.65, 11.87. X-ray quality single crystals were grown by slow diffusion of diethylether into an ethanol solution of **8**.

2.2.10. Catalytic Heck reactions

In a schlenk tube, iodobenzene (30 mmol) and hexamethylbenzene (100 mg, internal standard) were dissolved in 10 mL of DMF, under an inert atmosphere. The solution was heated up to 100 °C, then the olefin (36 mmol), K_2CO_3 (36 mmol) and the catalyst (0.3 mmol) were added and the progress of the reaction was monitored at GC–MS.

2.3. X-ray diffraction analysis

Crystals of complexes $[\text{Co}(\text{N},\text{O}-\text{L}^{\text{Ph}})_2]$ $\text{C}_2\text{H}_4\text{Cl}_2$ (**1** $\text{C}_2\text{H}_4\text{Cl}_2$) and $[\text{Pd}(\text{N},\text{O}-\text{L}^{\text{Me}})_2]$ (**8**) were mounted on a Stoe Image Plate Diffraction system equipped with a ϕ circle goniometer, using Mo-K α graphite monochromated radiation ($\lambda = 0.71073$ Å) with ϕ range 0–200°. The structures were solved by direct methods using the program SHELXS-97, while the refinement and all further calculations were carried out using SHELXL-97 [46]. Examination of the structure of complex **8** by PLATON [47] revealed a void of 87 Å³. This void was considered to be a highly disordered ethanol molecule, which was removed using the squeeze algorithm from PLATON. Otherwise, in both structures the H-atoms were included in calculated positions and treated as riding atoms using the SHELXL default parameters, while the non-H atoms were refined anisotropically, using weighted full-matrix least-square on F^2 . Crystallographic details are summarized in Table 1. Figs. 1 and 2 were drawn with ORTEP [48].

Table 1

Crystallographic and structure refinement parameters for complexes $[\text{Co}(\text{N},\text{O}-\text{L}^{\text{Ph}})_2]$ $\text{C}_2\text{H}_4\text{Cl}_2$ (**1** $\text{C}_2\text{H}_4\text{Cl}_2$) and $[\text{Pd}(\text{N},\text{O}-\text{L}^{\text{Me}})_2]$ (**8**).

	1	8
Chemical formula	$\text{C}_{40}\text{H}_{30}\text{Cl}_2\text{CoN}_4\text{O}_2$	$\text{C}_{26}\text{H}_{22}\text{N}_4\text{O}_2\text{Pd}$
Formula weight	728.51	552.90
Crystal system	monoclinic	monoclinic
Space group	C_2/c (No. 15)	$P 2_1/c$ (No. 14)
Crystal color & shape	brown block	orange block
Crystal size	$0.18 \times 0.16 \times 0.16$	$0.21 \times 0.19 \times 0.18$
a (Å)	23.8034(8)	11.0865(7)
b (Å)	12.9487(5)	7.5203(3)
c (Å)	11.3680(4)	16.6150(12)
β (°)	90	90
γ (°)	113.368(2)	116.943(5)
γ (°)	90	90
V (Å ³)	3216.5(2)	1234.90(13)
Z	4	2
T (K)	173(2)	173(2)
D_c ($\text{g}\cdot\text{cm}^{-3}$)	1.504	1.487
(mm^{-1})	0.745	0.784
Scan range (°)	$1.83 < 2\theta < 25.10$	$2.06 < 2\theta < 25.15$
Unique reflections	2867	2194
Reflections used $[I \geq 2\sigma(I)]$	2406	1537
R_{int}	0.0461	0.0805
Final R indices $[I \geq 2\sigma(I)]$	0.0317, wR_2 0.0802	0.0406, wR_2 0.0774
R indices (all data)	0.0401, wR_2 0.0837	0.0780, wR_2 0.0890
Goodness-of-fit	1.052	1.061
Max, Min $ e $ (Å ⁻³)	0.463, −0.463	0.375, −0.515

^aStructures were refined on F_0^2 : $wR_2 = [\sum(w(F_0^2 - F_c^2)^2) / \sum w(F_0^2)^2]^{1/2}$, where $w^{-1} = [\sum(F_0^2) + (aP)^2 + bP]$ and $P = [\max(F_0^2, 0) + 2F_c^2]/3$.

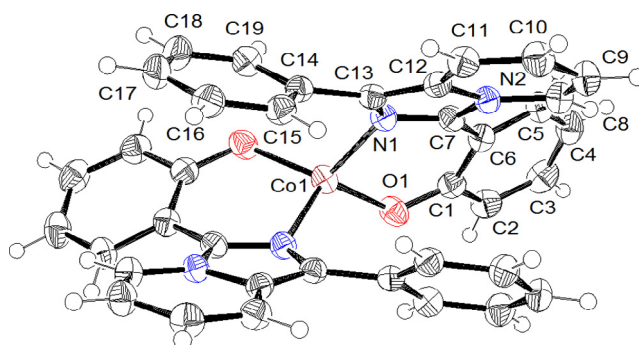


Fig. 1. ORTEP representation of $[\text{Co}(\text{N},\text{O}-\text{L}^{\text{Ph}})_2]$ at 50% probability level. Selected bond lengths (Å) and angles (°): Co(1)–N(1) 2.011(2), Co(1)–O(1) 1.894(2); N(1)–Co(1)–N(1)ⁱ 104.48(9), N(1)–Co(1)–O(1) 95.95(6), O(1)–Co(1)–O(1)ⁱ 126.19(9), N(1)–C(13)–C(14)–C(19)–39.2(3), N(1)–C(7)–C(6)–C(1)–32.1(3), O(1)–C(1)–C(6)–C(7) 7.38(3) ($i = -x, y, 0.5 - z$).

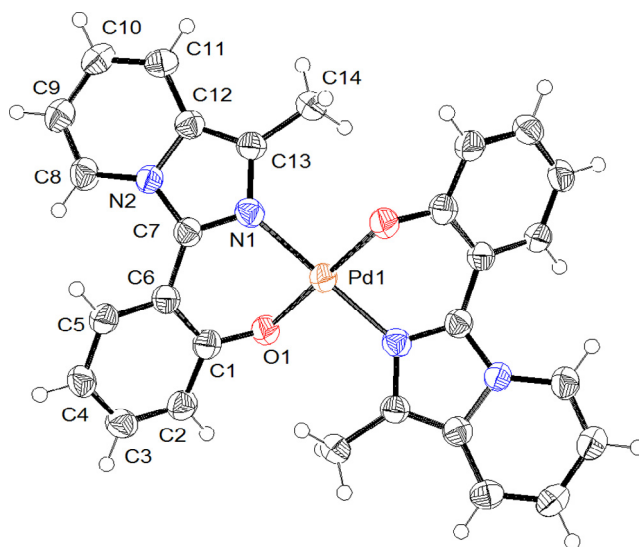


Fig. 2. ORTEP representation of $[\text{Pd}(\text{N},\text{O}-\text{L}^{\text{Me}})_2]$ at 50% probability level. Selected bond lengths (Å) and angles (°): Pd(1)–N(1) 2.034(4), Pd(1)–O(1) 2.011(3); N(1)–Pd(1)–O(1) 86.6(1), O(1)–Pd(1)–N(1)ⁱ 93.4(1); N(1)–C(7)–C(6)–C(1) 32.1(3), N(1)–C(7)–N(2)–C(8) 174.4(4) ($i = -x, 1 - y, -z$).

CCDC-1556974 $[\text{Co}(\text{N},\text{O}-\text{L}^{\text{Ph}})_2]$ $\text{C}_2\text{H}_4\text{Cl}_2$ (**1** $\text{C}_2\text{H}_4\text{Cl}_2$) and 1556975 $[\text{Pd}(\text{N},\text{O}-\text{L}^{\text{Me}})_2]$ (**8**) contain the supplementary crystallographic data for this paper. These data can be obtained free of charge at www.ccdc.cam.ac.uk/conts/retrieving.html [or from the Cambridge Crystallographic Data Centre, 12, Union Road, Cambridge CB2 1EZ, UK; fax: (internat.) +44-1223/336-033; E-mail: deposit@ccdc.cam.ac.uk].

2.4. Computational details

All calculations were carried out at the density functional (DFT) level of theory with the ADF2017.105 program package [49–51]. The hybrid functional PBE0 [52–54] was employed for geometry optimization. The PBE0 exchange correlation functional is based on the generalized gradient corrected exchange correlation functional by Perdew–Burke–Ernzerhof (PBE) [52–54] with a fixed amount of 25% of Hartree–Fock exchange energy. C, H, N, and O atoms were described through TZ2P basis sets [triple- ζ Slater-type orbitals (STOs) plus two polarization function]; the QZ4P basis set (quadruple- ζ STO plus four polarization functions) was used for the Pd atom. Scalar relativistic effects on palladium atoms were treated

ted by applying the zeroth-order regular approximation (ZORA) [55,56]. Restricted formalism, no-frozen-core approximation (all-electron) and no-symmetry constrains were used in all calculations. Complexes geometries were optimized simulating solvent effects (ethanol, CH_2Cl_2) employing the conductor-like continuum solvent model (COSMO) [57–59] as implemented in the ADF suite. Frequency calculations were performed for all optimized structures to establish the minima nature of stationary points.

3. Results and discussion

3.1. Syntheses and spectroscopic characterization

Ligand 2-(1-phenylimidazo[1,5-*a*]pyridin-3-yl)phenol ($\text{N,OH-L}^{\text{Ph}}$) (Scheme 1) was obtained as a light yellow powder according to a published procedure [45,27] and its purity was assessed by ^1H NMR and elemental analysis. The same procedure was initially applied to the synthesis of 2-(1-methylimidazo[1,5-*a*]pyridin-3-yl)phenol ($\text{N,OH-L}^{\text{Me}}$) (Scheme 1), by simply replacing 2-benzoylpyridine with 2-acetylpyridine, but a mixture of undefined products was systematically isolated. This was probably due to the high temperature involved. Therefore, we performed the reaction at room temperature, and optimized the working conditions by extending the reaction time to one week. By doing so, ligand $\text{N,OH-L}^{\text{Me}}$ was obtained as a pure orange solid in very high yield.

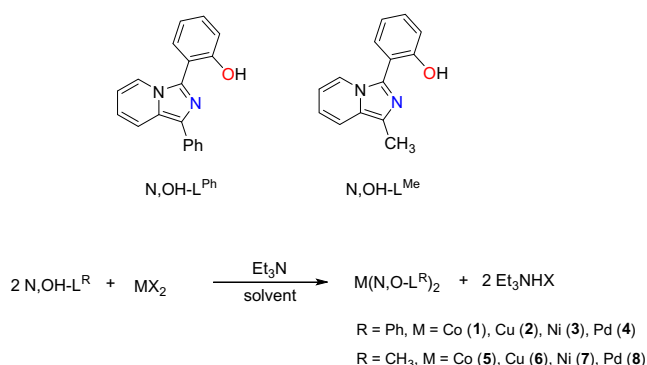
Complexes **1–8** have been prepared following similar procedures (Scheme 1), by reacting ligand N,OH-L^{R} with the corresponding metal(II) salt, in acetonitrile ($\text{M} = \text{Co}, \text{Cu}, \text{Ni}$) or in dichloromethane ($\text{M} = \text{Pd}$), at room temperature, in the presence of Et_3N . They are formulated respectively as $[\text{Co}(\text{N,OH-L}^{\text{Ph}})_2]$ (**1**), $[\text{Cu}(\text{N,OH-L}^{\text{Ph}})_2]$ (**2**), $[\text{Ni}(\text{N,OH-L}^{\text{Ph}})_2]$ (**3**), $[\text{Pd}(\text{N,OH-L}^{\text{Ph}})_2]$ (**4**), $[\text{Co}(\text{N,OH-L}^{\text{Me}})_2]$ (**5**), $[\text{Cu}(\text{N,OH-L}^{\text{Me}})_2]$ (**6**), $[\text{Ni}(\text{N,OH-L}^{\text{Me}})_2]$ (**7**), $[\text{Pd}(\text{N,OH-L}^{\text{Me}})_2]$ (**8**) (Scheme 1). All complexes are air and moisture stable, and have been characterized by elemental analysis and infrared spectroscopy. In their infrared spectra recorded with ATR-IR technique (Supplementary Material, Fig. S1–S8), they show the typical pattern of the coordinated ligands, with sharp and intense stretching bands in the region $1515\text{--}1615\text{ cm}^{-1}$ and an additional band of medium intensity around 1630 cm^{-1} ($\nu_{\text{C=N}}$). Furthermore, in the case of $\text{N,OH-L}^{\text{Me}}$ derivatives **5–8**, the $\nu_{\text{C=H}}$ stretchings of the methyl group are detected in the $2900\text{--}3100\text{ cm}^{-1}$ region.

As expected, due to the presence of the paramagnetic $\text{M}(\text{II})$ ion the NMR spectra recorded for the cobalt (**1** and **5**) and copper (**2** and **6**) derivatives are characterized by broad and undefined signals, often spread out over a wide spectral window (Figs. S9–S10 and S14–S15). A similar pattern is observed also for the nickel

compounds **3** and **7** (Figs. S11 and S16). In this case, both square planar and tetrahedral geometry around nickel(II) could be possible according to the proposed stoichiometry of the complexes. The broad signals in the NMR spectrum suggest a paramagnetic scenario for the nickel center, which consequently denotes a tetrahedral geometry in both complexes. Also the NMR investigation on the palladium complexes revealed interesting information about the nature of these compounds. The ^1H NMR spectrum of $[\text{Pd}(\text{N,OH-L}^{\text{Ph}})_2]$ (**4**) (Figs. S12–S13) is characterized by a complex pattern in the aromatic region: we attributed such a behavior to the presence of two isomers, respectively designated as *cis*- $[\text{Pd}(\text{N,OH-L}^{\text{Ph}})_2]$, *cis*-(**4**), and *trans*- $[\text{Pd}(\text{N,OH-L}^{\text{Ph}})_2]$, *trans*-(**4**), which originate from the possible mutual disposition of nitrogen and oxygen binding atoms of the two ligand molecules. Unfortunately, the complexity of the pattern did not allow a real quantification of the two isomers in solution. A similar (but better) situation has been observed for the methyl-containing derivative $[\text{Pd}(\text{N,OH-L}^{\text{Me}})_2]$ (**8**). Again, the presence of two possible isomers, *cis*-(**8**) and *trans*-(**8**), has been detected, this time with a definitely higher predominance of one species. Indeed, a combined 1D and 2D analysis including (Figs. S19–S20) allowed to identify all the signals belonging to the major isomer in solution (CD_2Cl_2 , $25\text{ }^\circ\text{C}$). From the integration of peaks area in ^1H NMR, we approximately calculated a major:minor isomer ratio of 4:1. DFT calculations performed on complexes *cis*-(**8**) and *trans*-(**8**) (see section 3.3) later supported the possibility to have a mixture of the two isomers in solution.

3.2. X-ray crystal structures

Two complexes, namely $[\text{Co}(\text{N,OH-L}^{\text{Ph}})_2]$ (**1**) and $[\text{Pd}(\text{N,OH-L}^{\text{Me}})_2]$ (**8**), were characterized via single-crystal X-ray structure analysis (Figs. 1 and 2). As expected, in both structures the two N,OH-L^{R} ligands are bound in a *N,O*-bidentate coordination mode via the deprotonated phenolic oxygen and the pyridine-like nitrogen of the imidazo-part (N_{im}) of the ligand. The molecular structures of complexes **1** and **8** are quite different from those observed for other $\text{M}(\text{II})$ ($\text{M} = \text{Co}, \text{Zn}$) derivatives bearing a 2-(imidazo[1,5-*a*]pyridin-3-yl)phenol ligand [60]. Indeed, in that case the absence of any substituent in position 1 of the imidazo[1,5-*a*]pyridine scaffold led to di- or trinuclear complexes, with the deprotonated ligand often bridging two adjacent metal centers. In our case, the presence of the methyl or the phenyl residue increased the steric hindrance of the ligand, thus most probably forcing the formation of mononuclear species. Consequently, in compounds **1** and **8** the metal centers are in a four coordinated *N,O,N,O* environment. In



Scheme 1. Imidazo[1,5-*a*]pyridine-based ligands used in this study (top) and syntheses of the $\text{M}(\text{II})$ complexes (bottom).

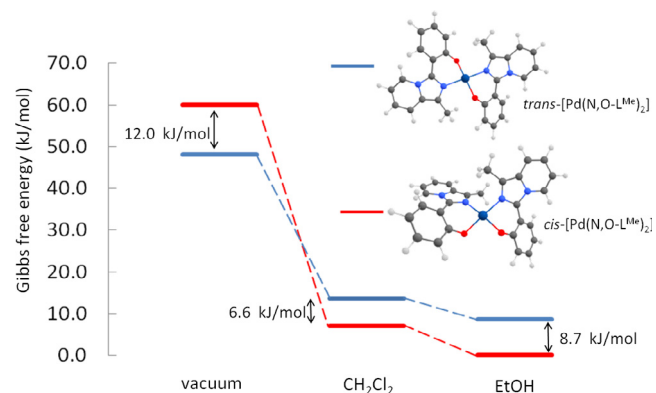


Fig. 3. Differences in Gibbs free energies for the optimized structures of *cis*- $[\text{Pd}(\text{N,OH-L}^{\text{Me}})_2]$ (*cis*-(**8**)) and *trans*- $[\text{Pd}(\text{N,OH-L}^{\text{Me}})_2]$ (*trans*-(**8**)) in vacuum, in CH_2Cl_2 and in ethanol.

[Co(N,O-L^{Ph})₂], the Co-N and Co-O bond distances measure respectively 2.011(2) and 1.894(2) Å, whereas angles around the cobalt atom are representative of a tetrahedral geometry (N(1)-Co(1)-N(1) = 104.48(9)°, N(1)-Co(1)-O(1) = 95.95(6)°, O(1)-Co(1)-O(1) = 126.19(9)°). Indeed, by applying the equation proposed by Houser [61] to these angles, a τ_4 value of 0.917 is obtained, thus speaking for a nearly ideal tetrahedral geometry for cobalt. Dihedral angles show that the phenyl-imidazo[1,5-*a*]pyridine moiety of the N,O-L^{Ph} ligand is quite far from a planar configuration: the C(12)-C(13)-C(14)-C(19) torsion angle being 140.3(2)°. The phenolic ring in position 3 of the imidazo[1,5-*a*]pyridine rotates along the C(13)-C(14) bond, and the two planes containing the 3-aryl and the imidazo-pyridine skeleton being twisted by 39.1°.

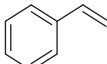
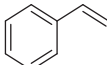
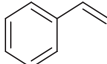
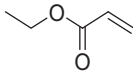
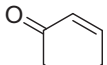
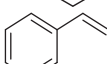
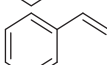
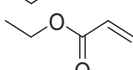
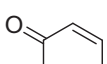
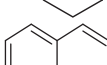
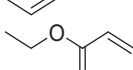
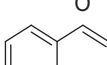
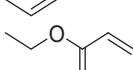
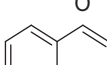
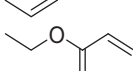
In [Pd(N,O-L^{Me})₂] (**8**) (Fig. 2), the palladium center is in a square planar environment comprising two phenolic oxygen and two nitrogen atoms from the two imidazo[1,5-*a*]pyridine ligands. The

oxygen atoms of the phenolic residue are in a *trans* configuration around the metal center. The Pd-N and Pd-O bond distances are 2.034(4) and 2.011(3) Å respectively, whereas basal angles designate a perfect square planar geometry around the palladium (N(1)-Pd(1)-N(1) = 180.0(2)°, O(1)-Pd(1)-O(1) = 180.0(2)°, O(1)-Pd(1)-N(1) = 93.4(1)°, N(1)-Pd(1)-O(1) = 86.6(1)°). Like complex **1**, the dihedral angles in **8** show that the phenyl-imidazo[1,5-*a*]pyridine moiety of the N,O-L^{Me} ligands is quite distorted from a planar configuration, the angle between the plane of the phenolate and the plane of the imidazo-pyridine skeleton being 37.7°.

3.3. DFT study on Pd(II) derivatives

The molecular structure of both *cis* and *trans* isomers of complexes [Pd(N,O-L^{Me})₂] (**8**) and [Pd(N,O-L^{Ph})₂] (**4**), *cis*-(**8**), *trans*-(**8**), *cis*-(**4**) and *trans*-(**4**), have been optimized at the Density Functional

Table 2
Outcomes of Heck reaction catalyzed by complexes [Pd(N,O-L^{Ph})₂] (**4**) and [Pd(N,O-L^{Me})₂] (**8**).^a

Entry	cat.	olefin	solvent	T (°C)	t (h)	Olefin Conversion (%) ^b	A (%)	B (%)	C (%)
1	8		THF	70	25	<5%	–	–	–
2	8		DMF	70	25	24%	94	6	–
3	8		DMF	100	15	95%	95	5	–
4	8		DMF	100	2.5	98%	100	–	–
5	8		DMF	100	8	99%	4	–	96
6 ^c	8		DMF	100	15	95%	94	6	–
7	4		DMF	100	30	90%	95	5	–
8	4		DMF	100	20	95%	100	–	–
9	4		DMF	100	25	95%	7	–	93
10	5		DMF	100	30	<5%	–	–	–
11	5		DMF	100	30	10%	97	3	–
12	6		DMF	100	30	<5%	–	–	–
13	6		DMF	100	30	<5%	–	–	–
14	7		DMF	100	30	15%	95	5	–
15	7		DMF	100	30	32%	98	2	–

^a General conditions: cat.: iodobenzene; olefin = 0.3: 30: 36 (mmol). Base: K₂CO₃ (36 mmol). Solvent: 10 mL.

^b Olefin conversion determined by GC-MS analysis (internal standard: hexamethylbenzene).

^c Bulk reaction filtered on Celite after complete conversion.

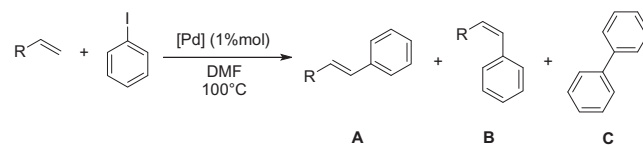
level of Theory (DFT) using the PBE0 [52–54] functional. All optimized structures (Supplementary Information) are minima in the potential surface of the molecule, as the calculation of the Hessian gave no imaginary frequencies. Concerning *cis*-(**8**) and *trans*-(**8**), there are no large differences between the gas-phase structures and those calculated in the presence of solvent (CH₂Cl₂ and ethanol). The largest deviation among bond distances is about 0.01 Å, while those of bond angles are less than 1°. Thermodynamic data obtained from frequencies analysis demonstrated that in the absence of any solvent interactions (*i.e.*, in the gas phase) the *trans* isomer is slightly more stable (Fig. 3), the difference ($G_{trans} - G_{cis}$) at 298 K being about 12 kJ/mol. In solution the situation slightly changes: indeed, in CH₂Cl₂ the *cis*- form becomes more stable by 6.6 kJ/mol (Fig. 3) and in the more polar ethanol the stabilization of *cis*-(**8**) with respect to *trans*-(**8**) is even superior (9 kJ/mol). The plausible reason for this variation is the high dipole moment of *cis*-(**8**) ($\mu_{cis} = 14.2$ D) compared to the absence of dipole moment shown by *trans*-(**8**) (*cis*-(**8**) adopts a C₁ symmetry, whereas *trans*-(**8**) has a C_i symmetry). Hence, a greater stability is expected for *cis*-(**8**) in polar solvents according to μ , as effectively attained by DFT calculations.

However, the energy difference between *cis*-(**8**) and *trans*-(**8**) is quite small, thus the isolation of the *cis* or *trans* isomer could be attributed to small differences in the reaction and precipitation conditions, with both isomers co-existing in solution. Indeed, a careful inspection of the ¹H NMR spectrum of complex **8** (see section 3.1) reveals the presence of a mixture of isomers with one isomer present only in an extremely minor fraction. Then, we can conclude that the crystallographic characterization of the *trans* isomer may merely be attributed to solid-state effects, with both isomers co-existing in solution. A similar situation was also found for the two possible isomers of [Pd(N,O-L^{Ph})₂] (**4**), namely *cis*-(**4**) and *trans*-(**4**). In this case, *cis*-(**4**) appears to be the more stable species in the absence or presence of solvents (Fig. S21). These observations are in accordance with the NMR outcomes discussed above.

3.4. Catalytic Heck reactions

The catalytic activity in the Heck reaction of complexes **1–8** was explored (Table 2), starting with the palladium(II) derivatives [Pd(N,O-L^{Ph})₂] (**4**) and [Pd(N,O-L^{Me})₂] (**8**). Iodobenzene was employed as the reference aryl halide, whereas the olefin was varied from styrene, 2-cyclohexen-1-one and ethyl acrylate (Scheme 2).

The reaction conditions (solvent, temperature) were optimized using styrene as substrate (entry 1–3), potassium carbonate as base and compound **8** as catalyst: DMF was chosen as solvent, and the reaction temperature was fixed at 100 °C. Under these conditions (entry 3), styrene was converted in the expected *trans*-stilbene with 95% selectivity, with no formation of biphenyl by-product. A similar result was obtained using ethyl acrylate as substrate (entry 4); in this case, the reaction time was shorter (2.5 h) compared to entry 3 (15 h). A different behavior was observed in the case of 2-cyclohexen-1-one (entry 5), with a scarce conversion to the desired substituted olefin, biphenyl being the main by-product. This can probably be ascribed to the higher steric hindrance of the internal olefin with respect to the terminal ones. Worthy of note, at the end of the reaction some palladium black was noticed in the bulk. Thus, it is not excluded that the homo-coupling reaction of iodobenzene leading to biphenyl was promoted by this Pd(0) species somehow generated in the course of the reaction. Then, an additional run was performed (entry 6) to rule out the possibility that also reactions in entry 1–4 were catalyzed by Pd(0). Indeed, the same conditions as in entry 3 were applied, and after completion of the reaction the bulk was filtered over a pad of Celite. Notably, no traces of palladium black were recovered after filtration, excluding the generation of palladium black in the catalytic runs



Scheme 2. Coupling of iodobenzene with different olefins catalyzed by complexes [Pd(N,O-L^{Ph})₂] (**4**) and [Pd(N,O-L^{Me})₂] (**8**).

1–4 and consequently supporting the active role played by compound **8** in entries 1–4. Similar results were then reached using complex [Pd(N,O-L^{Ph})₂] (**4**) as catalyst, with the exception of longer reaction times needed than in previous runs. This effect is reasonably due to the residue in position 1 of the imidazo-pyridine skeleton in ligand N,O-L^{Ph}: the phenyl substituent is less electron-donating than the methyl in N,O-L^{Me}, and this disfavor both the oxidative addition and the reductive elimination steps in the catalytic cycle [14].

With these outcomes in hands, we next tested the catalytic activity of the other methyl-containing complexes, [Co(N,O-L^{Me})₂] (**5**), [Cu(N,O-L^{Me})₂] (**6**) and [Ni(N,O-L^{Me})₂] (**7**), employing the same conditions as before. Despite all the reactions were performed at high temperatures (100 °C) and for prolonged times (30 h), complexes **5**, **6** and **7** showed poor catalytic activity. The cobalt derivative resulted only slightly active in the conversion of ethyl acrylate (entry 11), whereas no activity was noticed with styrene as substrate (entry 10). [Cu(N,O-L^{Me})₂] did not show catalytic activity, the products of the Heck reaction being recovered only in traces (entries 12–13) regardless the olefin used. Finally, species **7** could catalytically convert both the olefins in the desired products (entries 14–15), but the yields was satisfactory only with ethyl acrylate as substrate.

4. Conclusions

In this study, two imidazo[1,5-*a*]pyridine-based ligands (designated as N,OH-L^{Ph} and N,OH-L^{Me}) have been prepared and reacted with different divalent metals (M = Co, Cu, Ni, Pd). The corresponding complexes have been characterized by elemental analysis and infrared spectroscopy. ¹H NMR investigation allowed to confirm the paramagnetic nature of Co, Cu and Ni compounds, whereas ¹H and ¹³C NMR were used to shed light on the palladium derivatives. Two of these complexes, namely [Co(N,O-L^{Ph})₂] (**1**) and [Pd(N,O-L^{Me})₂] (**8**), were characterized via X-ray single crystal diffraction. The imidazo[1,5-*a*]pyridine ligand is *N,O*-coordinated via the pyridine-like nitrogen of the imidazo[1,5-*a*]pyridine skeleton (N_{im}) and the phenolic oxygen. Differently from what was observed for other reported M(II) compounds bearing similar *N,O*-bidentate imidazo[1,5-*a*]pyridine ligands (with H in position 1), in our case the ligands were not bridging two adjacent metal centers, but forming mononuclear species. This is most likely related to the increased steric hindrance given by the residue (Me or Ph) in position 1 of the heterocyclic moiety. TD-DFT calculations performed on the two possible isomers of compounds [Pd(N,O-L^{Me})₂] and [Pd(N,O-L^{Ph})₂] allowed to establish the relative energies of the different isomers. Finally, some compounds, namely [Co(N,O-L^{Me})₂], [Cu(N,O-L^{Me})₂], [Ni(N,O-L^{Me})₂], [Pd(N,O-L^{Me})₂] and [Pd(N,O-L^{Ph})₂] have been tested as catalysts in the Heck reaction between iodobenzene and different olefins, giving high yields of conversion in the case of palladium derivatives.

Acknowledgments

This work was supported by the Ministero dell'Università e della Ricerca (MIUR) and the University of Insubria (grant CSR-12).

Appendix A. Supplementary data

Supplementary data associated with this article can be found in the online version, at <https://doi.org/10.1016/j.ica.2017.11.039>.

References

- [1] R.F. Heck, J.P. Nolley, *J. Org. Chem.* 37 (1972) 2320–2322.
- [2] T. Mizoroki, K. Mori, A. Ozaki, *Bull. Chem. Soc. Jpn.* 44 (1971) 581.
- [3] H.-J. Xu, Y.-Q. Zhao, X.-F. Zhou, *J. Org. Chem.* 76 (2011) 8036–8041.
- [4] E.W. Werner, M.S. Sigman, *J. Am. Chem. Soc.* 133 (2011) 9692–9695.
- [5] C. Wu, J. Zhou, *J. Am. Chem. Soc.* 136 (2014) 650–652.
- [6] E. Coia, N. Sotomayor, E. Lete, *Adv. Synth. Catal.* 356 (2014) 1853–1865.
- [7] D. Mc Cartney, P.J. Guiry, *Chem. Soc. Rev.* 40 (2011) 5122–5150.
- [8] W. Kong, Q. Wang, J. Zhu, *Angew. Chem. Int. Ed.* 56 (2017) 3987–3991.
- [9] S. Mannathan, S. Raoufoghaddam, J.N.H. Reek, J.G. de Vries, A.J. Minnaard, *ChemCatChem* 9 (2017) 551–554.
- [10] A. Jutand, in: M. Oestreich (Ed.), *The Mizoroki-Heck Reaction*, Wiley & Sons, John, 2009, pp. 1–50.
- [11] A.B. Dounay, L.E. Overman, *Chem. Rev.* 103 (2003) 2945–2964.
- [12] P. Srinivas, P.R. Likhari, H. Maheswaran, B. Sridhar, K. Ravikumar, M. Lakshmi Kantam, *Chem. Eur. J.* 15 (2009) 1578–1581.
- [13] M. Lakshmi Kantam, P. Srinivas, J. Yadav, P.R. Likhari, S. Bhargava, *J. Org. Chem.* 74 (2009) 4882–4885.
- [14] S.-S. Wang, G.-Y. Yang, *Catal. Sci. Technol.* 6 (2016) 2862–2876.
- [15] H. Wang, W. Xu, Z. Wang, L. Yu, K. Xu, *J. Org. Chem.* 80 (2015) 2431–2435.
- [16] E. Yamaguchi, F. Shibahara, T. Murai, *Chem. Lett.* 40 (2011) 939–940.
- [17] F. Shibahara, R. Sugiura, E. Yamaguchi, A. Kitagawa, T. Murai, *J. Org. Chem.* 74 (2009) 3566–3568.
- [18] F. Shibahara, E. Yamaguchi, A. Kitagawa, A. Imai, T. Murai, *Tetrahedron* 65 (2009) 5062–5073.
- [19] S.A. Siddiqui, T.M. Potewar, R.J. Lahoti, K.V. Srinivasan, *Synthesis* 17 (2006) 2849–2854.
- [20] C. Hamdouchi, J.D. Blas, M.D. Prado, J. Gruber, B.A. Heinz, V.J. Vance, *J. Med. Chem.* 42 (1999) 50–59.
- [21] J.C. Teulade, G. Grassy, J.P. Girard, J.P. Chapat, M.S. De Buochberg, *Eur. J. Med. Chem.* 13 (1978) 271–276.
- [22] M. Nakatsuka, T. Shimamura, *Jpn. Kokai Tokkyo JP* 2001035664, 2001; *Chem. Abstr.*, 134 (2001) 170632.
- [23] T. Tominaga, T. Kohama, A. Takano, *Jpn. Kokai Tokkyo JP* 2001006877 (2001); *Chem. Abstr.*, 134 (2001) 93136.
- [24] D. Kitasawa, T. Tominaga, A. Takano, *Jpn. Kokai Tokkyo JP* 2001057292 (2001); *Chem. Abstr.*, 134 (2001) 200276.
- [25] H. Nakamura, H. Yamamoto, *PCT Int. Appl. WO* 2005043630 (2005); *Chem. Abstr.*, 142 (2005) 440277.
- [26] G. Volpi, G. Magnano, I. Benesperi, D. Saccone, E. Priola, V. Gianotti, M. Milanesio, E. Conteroso, C. Barolo, G. Viscardi, *Dyes Pigments* 137 (2017) 152–164.
- [27] L. Salassa, A. Albertino, C. Garino, G. Volpi, C. Nervi, R. Gobetto, K.I. Hardcastle, *Organometallics* 27 (2008) 1427–1435.
- [28] C. Garino, T. Ruiu, L. Salassa, A. Albertino, G. Volpi, C. Nervi, R. Gobetto, K.I. Hardcastle, *Eur. J. Inorg. Chem.* (2008) 3587–3591.
- [29] M.D. Weber, C. Garino, G. Volpi, E. Casamassa, M. Milanesio, C. Barolo, R.D. Costa, *Dalton Trans.* 45 (2016) 8984–8993.
- [30] N. Kundu, S.M. Towsif Abtab, S. Kundu, A. Endo, S.J. Teat, M. Chaudhury, *Inorg. Chem.* 51 (2012) 2652–2661.
- [31] A.L. Guckian, M. Doering, M. Ciesielski, O. Walter, J. Hjelm, N.M. O'Boyle, W. Henry, W.R. Browne, J.J. McGarvey, J.G. Vos, *Dalton Trans.* (2004) 3943–3949.
- [32] A. Schmidt, N. Grover, T.K. Zimmermann, L. Graser, M. Cokoja, A. Pöthig, F.E. Kühn, *J. Catal.* 319 (2014) 119–126.
- [33] K. Li, J.-L. Niu, M.-Z. Yang, Z. Li, L.-Y. Wu, X.-Q. Hao, M.-P. Song, *Organometallics* 34 (2015) 1170–1176.
- [34] G.A. Ardizzoia, S. Brenna, S. Durini, B. Therrien, *Organometallics* 31 (2012) 5427–5437.
- [35] G.A. Ardizzoia, S. Brenna, B. Therrien, *Dalton Trans.* 41 (2012) 783–790.
- [36] G.A. Ardizzoia, S. Brenna, B. Therrien, *Eur. J. Inorg. Chem.* (2010) 3365–3371.
- [37] G.A. Ardizzoia, S. Brenna, F. Castelli, S. Galli, N. Masciocchi, *Inorg. Chim. Acta* 363 (2010) 324–329.
- [38] G.A. Ardizzoia, S. Brenna, S. Durini, I. Trentin, B. Therrien, *Dalton Trans.* 42 (2013) 12265–12273.
- [39] G.A. Ardizzoia, S. Brenna, S. Cenini, G. La Monica, N. Masciocchi, A. Maspero, *J. Mol. Catal. A: Chemical* 204–205 (2003) 333–340.
- [40] N. Masciocchi, G.A. Ardizzoia, G. La Monica, A. Maspero, S. Galli, A. Sironi, *Inorg. Chem.* 40 (2001) 6983–6989.
- [41] G.A. Ardizzoia, S. Brenna, F. Castelli, S. Galli, C. Marelli, A. Maspero, *J. Organomet. Chem.* 693 (2008) 1870–1876.
- [42] G.A. Ardizzoia, S. Brenna, S. Durini, B. Therrien, M. Veronelli, *Eur. J. Inorg. Chem.* (2014) 4310–4319.
- [43] G.A. Ardizzoia, S. Brenna, S. Durini, B. Therrien, *Polyhedron* 90 (2015) 214–220.
- [44] S. Durini, G.A. Ardizzoia, B. Therrien, S. Brenna, *New. J. Chem.* 41 (2017) 3006–3014.
- [45] J. Wang, L. Dyers Jr., R. Mason Jr., P. Amoyaw, R. Bu, *J. Org. Chem.* 70 (2005) 2353–2356.
- [46] G.M. Sheldrick, *Acta Cryst.*, A 64 (2008) 112–122.
- [47] A.L. Spek, *J. Appl. Cryst.* 36 (2003) 7–13.
- [48] L.J. Farrugia, *J. Appl. Cryst.* 30 (1997) 565.
- [49] G. te Velde, F.M. Bickelhaupt, E.J. Baerends, C. Fonseca Guerra, S.J.A. van Gisbergen, J.G. Snijders, T. Ziegler, *J. Comp. Chem.* 22 (2001) 931–967.
- [50] C. Fonseca Guerra, J.G. Snijders, G. te Velde, E.J. Baerends, *Theor. Chem. Acc.* 99 (1998) 391–403.
- [51] ADF2017, SCM, Theoretical Chemistry, Vrije Universiteit, Amsterdam, The Netherlands, <http://www.scm.com>. See Supplementary Material for complete reference.
- [52] J.P. Perdew, K. Burke, M. Ernzerhof, *Phys. Rev. Lett.* 77 (1996) 3865–3868; erratum: *J.P. Perdew, K. Burke, M. Ernzerhof, Phys. Rev. Lett.* 78 (1997) 1396.
- [53] J.P. Perdew, M. Ernzerhof, K. Burke, *J. Chem. Phys.* 105 (1996) 9982–9985.
- [54] C. Adamo, V. Barone, *J. Chem. Phys.* 110 (1999) 6158–6170.
- [55] E. van Lenthe, E.J. Baerends, J.G. Snijders, *J. Chem. Phys.* 101 (1994) 9783–9792.
- [56] E. van Lenthe, A. Ehlers, E.J. Baerends, *J. Chem. Phys.* 110 (1999) 8943–8953.
- [57] A. Klamt, G.J. Schürmann, *J. Chem. Soc., Perkin Trans. 2* (1993) 799–805.
- [58] A. Klamt, V. Jonas, *J. Chem. Phys.* 105 (1996) 9972–9981.
- [59] C.-C. Pye, T. Ziegler, *Theor. Chem. Acc.* 101 (1999) 396–408.
- [60] Q. Gao, Y. Chen, Y. Liu, C. Li, D. Gao, B. Wu, H. Li, Y. Li, W. Liu, W. Li, *J. Coord. Chem.* 67 (2014) 1673–1692.
- [61] L. Yang, D.R. Powell, R.P. Houser, *Dalton Trans.* (2007) 955–964.